

Macroscopic quantum tunneling of Bose-Einstein condensates with long-range interaction

Kai Marquardt, Pascal Wieland, Rolf Häfner, Holger Cartarius, Jörg Main, and Günter Wunner
Institut für Theoretische Physik 1, Universität Stuttgart, 70550 Stuttgart, Germany

(Dated: December 7, 2012)

The ground state of Bose-Einstein condensates with attractive particle interaction is metastable. One of the decay mechanisms of the condensate is a collapse by macroscopic quantum tunneling, which can be described by the bounce trajectory as solution of the time-dependent Gross-Pitaevskii equation in imaginary time. For condensates with an electromagnetically induced gravity-like interaction the bounce trajectory is computed with an extended variational approach using coupled Gaussian functions and simulated numerically exact within the mean-field approach on a space-time lattice. It is shown that the variational computations converge very rapidly to the numerically exact result with increasing number of Gaussians. The tunneling rate of the condensate is obtained from the classical action and additional parameters of the bounce trajectory. The converged variational and numerically exact results drastically improve by several orders of magnitude the decay rates obtained previously with a simple variational approach using a single Gaussian-type orbital for the condensate wave function.

PACS numbers: 03.75.Hh, 34.20.Cf, 34.80.Qb, 04.40.b

I. INTRODUCTION

The macroscopic occupation of the bosonic ground state of ultracold quantum gases has been predicted by Bose and Einstein. At least since the first realization of Bose-Einstein condensates (BECs) in 1995 [1–3] they are a central part of experimental and theoretical atomic physics. In a cold diluted Bose gas the particles interact via short-range contact interactions determined by the s-wave scattering length a , which can be experimentally varied with the help of Feshbach resonances. In addition long-range interactions exist, e.g., in dipolar condensates [4], or in condensates with an attractive $1/r$ interaction, which have been proposed to be electromagnetically induced with a setup of six laser triads [5]. The condensates are typically held in a harmonic trap, however, in case of an attractive $1/r$ interaction the BEC can be self-trapped [5, 6], which means that no external trap is needed.

When the scattering length of the contact interaction is varied, the stable ground state plus an unstable excited state of a BEC with attractive $1/r$ interaction are created in a tangent bifurcation at a critical scattering length $a = a_{\text{cr}}$ [6, 7]. Below the critical scattering length the contact interaction is so attractive that the condensate collapses and no stationary state does exist [8]. The collapse of the condensate, e.g., induced by thermal excitations [9–12], is also possible at scattering lengths above the bifurcation point. However, even without thermal excitations, i.e., at zero temperature $T = 0$, the ground state of the condensate is only a metastable state and can collapse by macroscopic quantum tunneling as long as the contact interaction is attractive. The process can be described by using the bounce trajectory as outlined by Stoof [13] and by Freire and Arovas [14].

The aim of the present paper is a thorough investigation and computation of the bounce trajectory of a BEC. It has been shown that the stationary states of

the GPE can be excellently described with an extended variational approach using coupled Gaussian functions [15, 16]. Here we will demonstrate that computations with coupled Gaussians are also a full-fledged alternative to simulations on a space-time lattice to obtain the bounce trajectory which describes the macroscopic quantum tunneling of the BEC. We apply the formalism to a self-trapped BEC with an attractive $1/r$ interaction. On the one hand the simplicity of this spherically symmetric system allows for an intuitive access to the bounce trajectory similar to the one-dimensional potential picture used by Stoof [13] and Freire et al. [14, 17]. On the other hand we can show that it is possible to include long-range interactions into the instanton formalism for BECs. The theory presented in this article can be applied to more realistic dipolar condensates [4] as well since their description does not contain a conceptual difference.

The paper is organized as follows. The basic concepts are briefly outlined in Sec. II. In Sec. III A the time-dependent variational principle (TDVP) is applied to an ansatz of coupled Gaussians for the wave functions in imaginary time. Periodic solutions of the equations of motion for the variational parameters are obtained by application of a multi-shooting algorithm, which converge with increasing period to the bounce trajectory. In Sec. III B the method for exact numerical simulations on space-time lattices is elaborated. The results of both methods are presented and compared in Sec. IV. Concluding remarks and an outlook are given in Sec. V.

II. BASIC CONCEPTS

For condensates without long-range interactions the macroscopic quantum tunneling has been investigated by Stoof [13] using a variational approach with a single Gaussian function as a simple approximation. For a self-

trapped BEC with an attractive $1/r$ interaction instead of an external harmonic potential the ideas outlined in Ref. [13] can briefly be summarized as follows. Starting from the many-body Schrödinger equation a mean-field approach leads to the time-dependent nonlinear Gross-Pitaevskii equation (GPE)

$$i \frac{d}{dt} \psi(\mathbf{r}, t) = [-\Delta + V_c(\mathbf{r}, t) + V_u(\mathbf{r}, t)] \psi(\mathbf{r}, t) \quad (1)$$

with the contact and long-range potentials

$$V_c(\mathbf{r}, t) = 8\pi N a |\psi(\mathbf{r}, t)|^2, \quad (2)$$

$$V_u(\mathbf{r}, t) = -2N \int d^3 r' \frac{|\psi(\mathbf{r}', t)|^2}{|\mathbf{r} - \mathbf{r}'|}, \quad (3)$$

where a is the scattering length, N is the number of bosons, and “natural” units [6] were used. Lengths are measured in units of $a_u = \hbar^2/(mu)$, energies in units of $E_u = \hbar^2/(2ma_u^2)$, and times in units of $t_u = \hbar/E_u$, where u determines the strength of the atom-atom interaction [5], and m is the mass of one boson. Exploiting the scaling properties presented in Ref. [6] and introducing the scaled variables

$$(\tilde{\mathbf{r}}, \tilde{a}, \tilde{t}, \tilde{\psi}) = (N\mathbf{r}, N^2a, N^2\tilde{t}, N^{-3/2}\psi) \quad (4)$$

the GPE keeps the form given in Eq. (1), however, with the particle number in the potentials V_c and V_u in Eqs. (2) and (3) formally set to $N = 1$. Note that the scaled GPE for the self-trapped BEC only depends on one parameter, viz. the scaled scattering length. In the following we use the scaled variables unless otherwise stated and omit the tilde.

Using a Gaussian-type orbital

$$\psi(r, t) = 4 \left[\frac{2}{3\pi q(t)^2} \right]^{3/4} \exp \left\{ \left[-\frac{4}{3q(t)^2} + i \frac{p(t)}{2q(t)} \right] r^2 \right\} \quad (5)$$

normalized to $\|\psi\|^2 = 1$ as a simple variational ansatz for the condensate wave function the TDVP can be applied, and it can be shown [8] that the parameters q and p obey the canonical equations of motion

$$\dot{q} = \frac{\partial H}{\partial p}, \quad \dot{p} = -\frac{\partial H}{\partial q}, \quad (6)$$

with the Hamiltonian $H(q, p) = p^2 + V(q)$ and the potential

$$V(q) = \frac{9}{4q^2} + \sqrt{\frac{3}{\pi}} \frac{3a}{2q^3} - \sqrt{\frac{3}{\pi}} \frac{1}{q}. \quad (7)$$

Important features of the BEC can be simply obtained, at least qualitatively, from the potential $V(q)$ shown in Fig. 1(a). For scattering lengths $a < a_{\text{cr}} = -3\pi/8 = -1.1781$ the potential $V(q)$ does not possess any stationary points, i.e., the condensate collapses. For $a_{\text{cr}} < a < 0$ two stationary points exist, the local minimum at $q =$

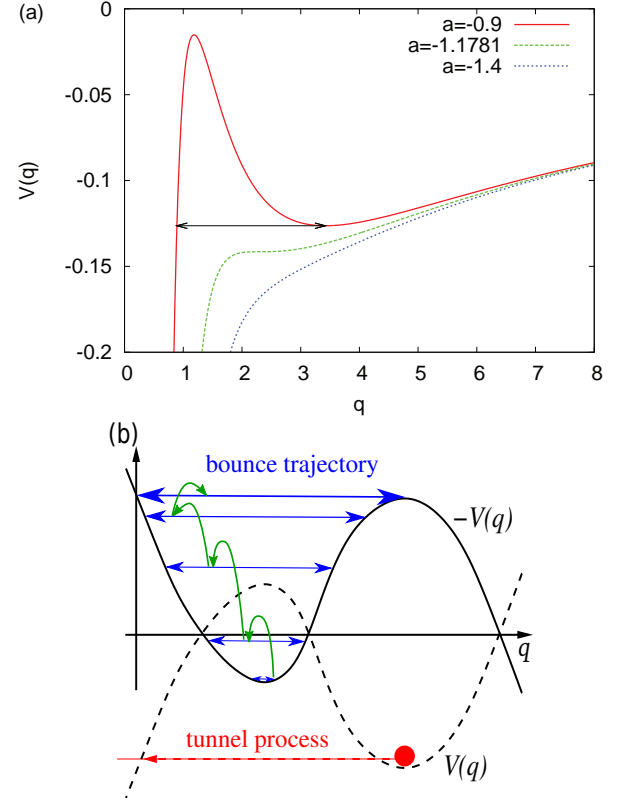


FIG. 1. (Color online) (a) Potential $V(q)$ of a self-trapped BEC with attractive $1/r$ interaction at various values of the scattering length a . (b) Scheme of the inversion of the potential and the periodic orbits approaching the bounce trajectory.

q_{\min} and maximum at $q = q_{\max}$ of the potential indicate the stable ground state and the unstable excited state, with $V(q_{\min})$ and $V(q_{\max})$ the mean-field energies $E_{\text{mf}} = \langle \psi | -\Delta + \frac{1}{2}(V_c + V_u) | \psi \rangle$ of the two states, respectively.

From Fig. 1(a) it is obvious that the potential $V(q)$ at small values of q drops below the mean-field energy of the ground state. The path through the potential barrier connecting the position of the ground state and the collapsing region [see the arrow in Fig. 1(a)] is classically forbidden. In quantum mechanics, however, the barrier can be crossed by a tunneling process, which is described by propagation along that path, called the bounce trajectory, in imaginary time. The decay rate of the metastable ground state depends on parameters of the bounce trajectory.

In the mean-field approach the many-body ground state is the product of N identical one-particle wave functions, and thus the collapse of a BEC requires the collective tunneling of all N bosons. As a consequence for macroscopic quantum tunneling an effective Planck constant \hbar/N must be used in the formula for the decay rate

Γ_0 . The final result derived by Stoof [13] reads

$$\Gamma_0 = \sqrt{\frac{Nm\omega_0 v_0^2}{\pi\hbar}} e^{-\frac{N}{\hbar} S_b} \quad (8)$$

where

$$S_b = 2 \int_{q_b}^{q_{\min}} \sqrt{V(q) - V(q_{\min})} dq \quad (9)$$

is the Euclidean action of the bounce trajectory (with the turning points q_b and q_{\min}) in imaginary time $it \rightarrow \tau$ running in the inverted potential (7), i.e., $V(q) \rightarrow -V(q)$ as illustrated in Fig. 1(b). The parameter ω_0 is the frequency of oscillations in the potential minimum around $q \approx q_{\min}$ given by

$$\omega_0 = \frac{1}{m} V''(q_{\min}), \quad (10)$$

and v_0 is defined by the condition that the bounce trajectory approaches the maximum of the inverted potential $-V(q)$ [see Fig. 1(b)] in the limit $\tau \rightarrow \pm\infty$ as

$$q(\tau) \sim q_{\min} - \frac{v_0}{\omega_0} e^{-\omega_0 |\tau|}. \quad (11)$$

The computation of the decay rate Γ_0 in Eq. (8) with the parameters S_b , ω_0 , and v_0 of the bounce trajectory as explained above is only a rough approximation for the following two reasons. Firstly, the ansatz with a single Gaussian function in Eq. (5) cannot describe the true condensate wave function. The variational solutions significantly deviate from those found in full numerical simulations even for the stationary ground and excited state [6, 7]. Secondly, the true solution of the GPE (1) can fluctuate around both the stationary ground state and the time-dependent bounce trajectory. The modes of these fluctuations are described, in leading order, by the Bogoliubov-de Gennes equations [18]. In Eq. (8) only fluctuations along the direction of the path are considered, i.e., for a system with only one degree of freedom. The true condensate wave function has many degrees of freedom, which allows for fluctuations perpendicular to the direction of the path. The fluctuation determinant resulting from those additional degrees of freedom is not accounted for by Eq. (8).

The method proposed by Stoof [13] requires the description of the bounce trajectory with canonical variables and the Hamiltonian formalism. Such a description is, however, restricted to a variational ansatz for the condensate wave function with a single Gaussian function as in Eq. (5), and thus any improvement of the simple variational approach is a nontrivial task.

A decisive step for the improvement of the bounce trajectory approach was achieved by Freire and Arovas [14]. They found a way to compute the bounce process beyond the interpretation in terms of a classical trajectory by applying the instanton formalism to a BEC in a harmonic trap without long-range interaction. The bounce trajectory was simulated numerically on a space-time lattice without any restriction to the wave function.

To solve the GPE (1) in imaginary time $it \rightarrow \tau$ the two fields $\psi(\mathbf{r}, \tau)$ and $\bar{\psi}(\mathbf{r}, \tau)$ are introduced, which obey the equations

$$-\frac{d}{d\tau} \psi(\mathbf{r}, \tau) = H\psi(\mathbf{r}, \tau), \quad \frac{d}{d\tau} \bar{\psi}(\mathbf{r}, \tau) = H\bar{\psi}(\mathbf{r}, \tau), \quad (12)$$

with

$$H(\mathbf{r}, \tau) = -\Delta + V_c(\mathbf{r}, \tau) + V_u(\mathbf{r}, \tau) - \mu, \quad (13)$$

$$V_c(\mathbf{r}, \tau) = 8\pi Na \bar{\psi}(\mathbf{r}, \tau) \psi(\mathbf{r}, \tau), \quad (14)$$

$$V_u(\mathbf{r}, \tau) = -2N \int d^3 r' \frac{\bar{\psi}(\mathbf{r}', \tau) \psi(\mathbf{r}', \tau)}{|\mathbf{r} - \mathbf{r}'|}. \quad (15)$$

Note that μ is a free parameter in Eq. (13) and the function $\bar{\psi}(\mathbf{r}, \tau)$ in imaginary time plays the role of the complex conjugate $\psi^*(\mathbf{r}, t)$ in real time dynamics. The probability density is given by $\bar{\psi}\psi$ and the norm defined by $\int \bar{\psi}(\mathbf{r}, \tau) \psi(\mathbf{r}, \tau) d^3 r$ is conserved. The bounce trajectory (with real valued ψ and $\bar{\psi}$) must fulfill the boundary conditions [14, 17]

$$\bar{\psi}(\mathbf{r}, \tau) = \psi(\mathbf{r}, -\tau), \quad (16)$$

$$\lim_{\tau \rightarrow \pm\infty} \bar{\psi}(\mathbf{r}, \tau) = \lim_{\tau \rightarrow \pm\infty} \psi(\mathbf{r}, \tau) \equiv \psi_g(\mathbf{r}), \quad (17)$$

with $\psi_g(\mathbf{r})$ the wave function of the stationary ground state. The Euclidean action of a periodic trajectory in imaginary time with period β is given by

$$S_e = \int_{-\beta/2}^{\beta/2} d\tau \int d^3 r \left\{ \bar{\psi} \frac{d}{d\tau} \psi - \mathcal{H} \right\}, \quad (18)$$

with the associated Hamiltonian density

$$\mathcal{H} = -\nabla \bar{\psi} \nabla \psi + 4\pi a (\bar{\psi} \psi)^2 - \int d^3 r' \frac{\psi' \bar{\psi}' \psi \bar{\psi}}{|\mathbf{r} - \mathbf{r}'|}. \quad (19)$$

Due to the symmetry (16) of ψ and $\bar{\psi}$ and the behavior of $S_e[q_b]$ and $S_e[q_0]$ the difference $\Delta S_e = S_e[q_b] - S_e[q_0]$ between the actions of the bounce trajectory and the fixed point is obtained as [14]

$$\Delta S_e = \int_0^{\beta/2} d\tau \int d^3 r \left\{ \bar{\psi} \frac{d}{d\tau} \psi - \psi \frac{d}{d\tau} \bar{\psi} \right\}. \quad (20)$$

Within the mean-field approach the formalism allows, in principle, for the exact computation of the bounce trajectory and related parameters needed as input for the calculation of the decay rate of the BEC in Eq. (8) without resort to the ansatz (5) and any canonical variables.

III. CALCULATION OF THE BOUNCE TRAJECTORY

The computation of the exact bounce trajectory which describes within the mean-field approach the macroscopic

quantum tunneling of a metastable BEC is the central issue of this paper. We first introduce in Sec. III A the extended variational approach with coupled Gaussian functions, and then in Sec. III B the numerical simulations on space-time lattices. The derivations are presented for a self-trapped BEC with attractive $1/r$ interaction, where the condensate wave function is spherically symmetric.

A. Variational approach with coupled Gaussians

The variational ansatz with a single Gaussian function in Eq. (5) cannot exactly reproduce the true condensate wave function. However, it has been shown that an extended variational approach with coupled Gaussians yields excellent results for both the stationary ground and excited state of the BEC [16]. Only very few (about three to five) coupled Gaussians are sufficient to achieve convergence of the wave function, the mean-field energy, and the chemical potential to those obtained in numerical computations on grids. We therefore will use a variational approach with coupled Gaussians also for the calculation of the bounce trajectory. For the dynamical calculations in imaginary time we write both functions ψ and $\bar{\psi}$ as superpositions of N_g Gaussian functions,

$$\psi(r, \tau) = \sum_{k=1}^{N_g} e^{-[A_k(\tau)r^2 + \gamma_k(\tau)]} \equiv \sum_{k=1}^{N_g} g_k, \quad (21a)$$

$$\bar{\psi}(r, \tau) = \sum_{k=1}^{N_g} e^{-[\bar{A}_k(\tau)r^2 + \bar{\gamma}_k(\tau)]} \equiv \sum_{k=1}^{N_g} \bar{g}_k. \quad (21b)$$

The $4N_g$ time-dependent variational parameters can be written as two vectors

$$\mathbf{z} = (A_1, \dots, A_{N_g}, \gamma_1, \dots, \gamma_{N_g}), \quad (22a)$$

$$\bar{\mathbf{z}} = (\bar{A}_1, \dots, \bar{A}_{N_g}, \bar{\gamma}_1, \dots, \bar{\gamma}_{N_g}). \quad (22b)$$

The equations of motion for the variational parameters \mathbf{z} and $\bar{\mathbf{z}}$ can be obtained using the TDVP of Dirac, Frenkel, and McLachlan [19, 20], which must be modified and adopted in a special way for the dynamics in imaginary time. In imaginary time the functional

$$I = \int d^3r [\bar{\phi} - H\bar{\psi}][\phi + H\psi] \quad (23)$$

must be minimized with respect to $\phi = \dot{\psi}$ and $\bar{\phi} = \dot{\bar{\psi}}$, with the Hamiltonian H given in Eq. (13). The dots now mark derivatives $d/d\tau$. With

$$\delta\phi = \sum_{k=1}^{2N_g} \left\{ \frac{\partial\psi}{\partial z_k} \delta\dot{z}_k \right\}, \quad \delta\bar{\phi} = \sum_{k=1}^{2N_g} \left\{ \frac{\partial\bar{\psi}}{\partial \bar{z}_k} \delta\dot{\bar{z}}_k \right\}, \quad (24)$$

we obtain the condition

$$\begin{aligned} \delta I &= \int d^3r \{ \delta\bar{\phi} [\phi + H\psi] + \delta\phi [\bar{\phi} - H\bar{\psi}] \} \\ &= \int d^3r \sum_{k=1}^{2N_g} \left\{ \left[(\phi + H\psi) \frac{\partial\bar{\psi}}{\partial \bar{z}_k} \right] \delta\dot{\bar{z}}_k \right. \\ &\quad \left. + \left[(\bar{\phi} - H\bar{\psi}) \frac{\partial\psi}{\partial z_k} \right] \delta\dot{z}_k \right\} = 0, \end{aligned} \quad (25)$$

and thus, because all $\delta\dot{z}_k$ and $\delta\dot{\bar{z}}_k$ are independent

$$\int d^3r \left[(\psi + H\psi) \frac{\partial\bar{\psi}}{\partial \bar{z}_k} \right] = 0, \quad (26a)$$

$$\int d^3r \left[(\bar{\psi} - H\bar{\psi}) \frac{\partial\psi}{\partial z_k} \right] = 0, \quad (26b)$$

for $k = 1, \dots, 2N_g$. Using the ansatz (21) with coupled Gaussians and the Hamiltonian (13) in Eq. (26) a calculation similar to that in Ref. [15] yields the equations of motion for the variational parameters

$$\dot{A}_k = -4A_k^2 + v_k^{(2)}, \quad (27a)$$

$$\dot{\gamma}_k = 6A_k + v_k^{(0)} - \mu, \quad (27b)$$

$$\dot{\bar{A}}_k = 4\bar{A}_k^2 - \bar{v}_k^{(2)}, \quad (27c)$$

$$\dot{\bar{\gamma}}_k = -6\bar{A}_k - \bar{v}_k^{(0)} + \mu, \quad (27d)$$

with $k = 1, \dots, N_g$. As in Eq. (13) μ is a free parameter, which becomes the chemical potential for stationary states. The parameters $v_k^{(2)}$, $v_k^{(0)}$, $\bar{v}_k^{(2)}$ and $\bar{v}_k^{(0)}$ in Eq. (27) are obtained by solving the two linear systems of equations

$$\sum_{k=1}^{N_g} v_k^{(0)} [1]_{lk} + \sum_{k=1}^{N_g} v_k^{(2)} [r^2]_{lk} = \sum_{k=1}^{N_g} [V]_{lk}, \quad (28a)$$

$$\sum_{k=1}^{N_g} v_k^{(0)} [r^2]_{lk} + \sum_{k=1}^{N_g} v_k^{(2)} [r^4]_{lk} = \sum_{k=1}^{N_g} [r^2 V]_{lk}, \quad (28b)$$

and

$$\sum_{k=1}^{N_g} \bar{v}_k^{(0)} [1]_{kl} + \sum_{k=1}^{N_g} \bar{v}_k^{(2)} [r^2]_{kl} = \sum_{k=1}^{N_g} [V]_{kl}, \quad (29a)$$

$$\sum_{k=1}^{N_g} \bar{v}_k^{(0)} [r^2]_{kl} + \sum_{k=1}^{N_g} \bar{v}_k^{(2)} [r^4]_{kl} = \sum_{k=1}^{N_g} [r^2 V]_{kl}, \quad (29b)$$

with $V = V_c + V_u$ and the notation

$$[O]_{lk} = \langle \bar{g}_l | O | g_k \rangle = \int d^3r \bar{g}_l O g_k. \quad (30)$$

All required integrals can be calculated analytically and are given in Appendix A.

The equations of motion (27) are a set of $4N_g$ ordinary differential equations, which can be integrated,

e.g., with a Runge-Kutta method. Because the period β of the bounce trajectory is infinite we start searching for periodic orbits, with the boundary conditions $\bar{\psi}(\tau = 0) = \psi(\tau = 0)$ and $\bar{\psi}(\tau = \beta/2) = \psi(\tau = \beta/2)$, near the excited state, as illustrated in Fig. 1(b), and then increase β . In the limit $\beta \rightarrow \infty$ the periodic orbits converge towards the bounce trajectory. The periodic orbit search could be performed, in principle, by varying the initial conditions of the variational parameters at $\tau = 0$ with $\bar{\psi}(0) = \psi(0)$ in such a way, that $\bar{\psi}(\beta/2) = \psi(\beta/2)$ is fulfilled at the other turning point. Numerically, however, this is an impossible task because the equations of motion are extremely unstable. The reason is that, e.g., for the ground state all stable modes of the Bogoliubov spectrum in real time become unstable modes in imaginary time, and thus all perturbations of the ground state (or a trajectory) increase exponentially in imaginary time. To overcome this problem we use a multi-shooting algorithm, where the trajectory is divided into small segments. Using M segments the total set of $4MN_g + 1$ parameters [including the parameter μ in the equations of motion (27)] can be determined to fulfill the $4MN_g$ continuity conditions of the variational parameters and the condition $\int d^3r \bar{\psi}\psi = 1$ for normalization by using a multidimensional Newton's method. Because the norm of $\bar{\psi}\psi$ is conserved, the total set of parameters can be slightly reduced by introducing the parameters $\tilde{\gamma}_k = \gamma_k - \gamma_1$ and $\tilde{\bar{\gamma}}_k = \bar{\gamma}_k - \bar{\gamma}_1$ for $k = 2, \dots, N_g$ instead of γ_k and $\bar{\gamma}_k$ for $k = 1, \dots, N_g$.

As an example Fig. 2 shows the variational parameters of a periodic trajectory at scaled scattering length $a = -0.9$ with period $\beta = 47.4$ near the bounce. The BEC is described by a superposition of $N_g = 3$ Gaussian functions. The high values of the parameters A_k and \bar{A}_k in Fig. 2(a) indicate a small width of the condensate wave function at the bounce around $\tau = 0$.

Once a bounce trajectory has been found improved values of the parameters S_b , ω_0 , and v_0 in the formula (8) for the decay rate of the BEC can be determined. The Euclidean action $S_b = \Delta S_e$ of a periodic trajectory is given in Eq. (20). For the ansatz with coupled Gaussians the action can directly be expressed in terms of the variational parameters,

$$\Delta S_e = \int_0^{\beta/2} d\tau \sum_{k,l=1}^{N_g} \left\{ \left(\dot{\bar{A}}_l - \dot{A}_k \right) \langle \bar{g}_l | r^2 | g_k \rangle + (\dot{\bar{\gamma}}_l - \dot{\gamma}_k) \langle \bar{g}_l | g_k \rangle \right\}. \quad (31)$$

The matrix elements are given in Eqs. (A1) and (A2) in Appendix A.

The frequency ω_0 is obtained, instead of using the potential in Eq. (10), by a stability analysis of the ground state. For the ansatz with coupled Gaussian functions the stability parameters are obtained as eigenvalues of the Jacobian matrix constructed by varying the variational parameters around the fixed point solution [15]. The eigenvalue ω_0 belongs to the variation of the param-

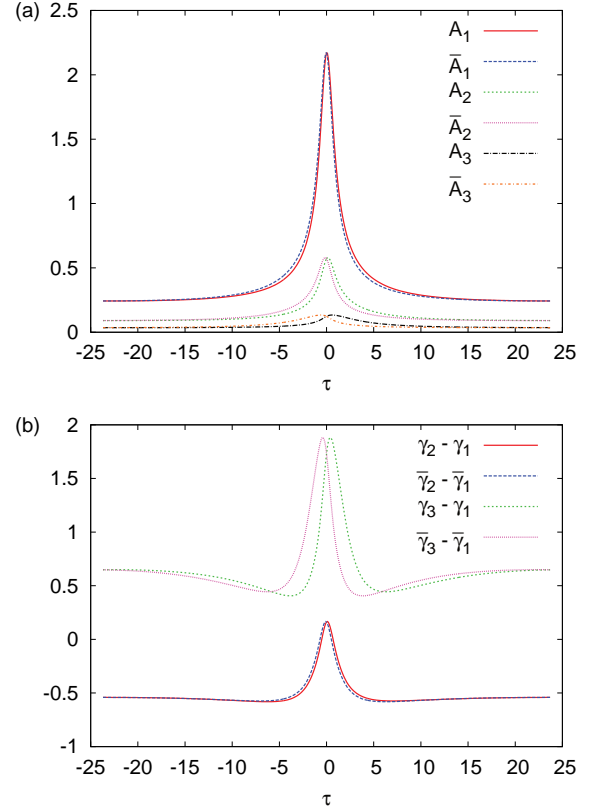


FIG. 2. (Color online) Variational parameters (a) $A_k(\tau)$, $\bar{A}_k(\tau)$ for $k = 1, \dots, N_g$ and (b) $\gamma_k(\tau) - \gamma_1(\tau)$, $\bar{\gamma}_k(\tau) - \bar{\gamma}_1(\tau)$ for $k = 2, \dots, N_g$ of a periodic trajectory with period $\beta = 47.4$ at scaled scattering length $a = -0.9$ described by $N_g = 3$ coupled Gaussian functions.

eters in the direction of the bounce trajectory.

The parameter v_0 cannot be determined using Eq. (11) because no canonical coordinate $q(\tau)$ exists for the ansatz with coupled Gaussians. However, when the bounce trajectory is approached via periodic orbits, v_0 can be estimated using the mean-field energies E_{mf}^g and $E_{\text{mf}}(\beta)$ of the ground state and periodic trajectories with period β . Using a model with an inverted harmonic potential for approaching the saddle in imaginary time we obtain (see Appendix B)

$$v_0 = \lim_{\beta \rightarrow \infty} \sqrt{\frac{E_{\text{mf}}(\beta) - E_{\text{mf}}^g}{2m}} e^{\omega_0 \beta/2}. \quad (32)$$

Results obtained with coupled Gaussians are presented in Sec. IV and compared with numerically exact simulations on space-time lattices.

B. Numerical simulations on space-time lattices

To verify the validity of the extended variational approach with coupled Gaussian functions we have carried out numerically exact computations by simulating the

bounce trajectory on a space-time lattice. Because the condensate wave function is spherically symmetric only the r coordinate needs to be discretized in space. We set $\psi_{i,j} \equiv \psi(i\Delta r, j\Delta\tau)$ and $\bar{\psi}_{i,j} \equiv \bar{\psi}(i\Delta r, j\Delta\tau)$ with $i = 1, \dots, m$ and $j = 1, \dots, n$ for an (m, n) space-time lattice with step sizes Δr and $\Delta\tau$, respectively.

The propagation in imaginary time is obtained with the operators

$$U = e^{-H\tau}, \quad \bar{U} = e^{H\tau}, \quad (33)$$

applied to the wave functions ψ and $\bar{\psi}$, respectively. The Hamiltonian $H = T + V_c + V_u - \mu$ is given in Eq. (13). Because the operators of the kinetic energy $T = -\Delta$ and of the potential $V = V_c + V_u$ do not commute we adopt the Baker-Hausdorff formula

$$e^{-(T+V)\Delta\tau} \approx e^{-V\Delta\tau/2} e^{-T\Delta\tau} e^{-V\Delta\tau/2}, \quad (34)$$

valid for small time steps $\Delta\tau$ and apply the split-operator method. The operators $e^{\pm V\Delta\tau/2}$ are applied in coordinate space, and the operators $e^{\pm T\Delta\tau}$ in momentum space. The Fourier transform of a spherically symmetric wave function $\psi(r)$ yields

$$\tilde{\psi}(k) = \mathcal{F}\{\psi(r)\} = \frac{4\pi}{k} \int_0^\infty r\psi(r) \sin(kr) dr, \quad (35)$$

which can be computed efficiently on the grid by a fast sine transform [21]. For the potential $V_u(r)$ of the attractive $1/r$ interaction [see Eq. (15)] we obtain by application of the convolution theorem

$$V_u(r) = \mathcal{F}^{-1} \left\{ \mathcal{F}\{\bar{\psi}\psi\} \mathcal{F} \left\{ \frac{1}{|r|} \right\} \right\} = \frac{8}{r} \int_0^\infty \frac{1}{k^2} \times \left[\int_0^\infty r' \bar{\psi}(r') \psi(r') \sin(kr') dr' \right] \sin(kr) dk, \quad (36)$$

where the integrals are also computed by fast sine transforms. For large values of r the potential $V_u(r)$ asymptotically approaches $-2/r$, however, the sine transform yields $V_u(r_{\max}) = 0$ at the border $r_{\max} = m\Delta r$ of the grid. The error is corrected by a shift of the potential $V_u(r) \rightarrow V_u(r) - 2/r_{\max}$.

The space-time lattice can be initialized, e.g., by discretizing a trajectory obtained with the extended variational approach introduced in Sec. III A. The remaining task is then to fulfill the matching conditions that the grid points of ψ and $\bar{\psi}$ at time $\tau = j\Delta\tau$ propagated by a time step $\Delta\tau$ coincide with the grid points of ψ and $\bar{\psi}$ at time $\tau = (j+1)\Delta\tau$. For a periodic trajectory furthermore the boundary conditions at the turning points $\bar{\psi}(\tau=0) = \psi(\tau=0)$ and $\bar{\psi}(\tau=n\Delta\tau) = \psi(\tau=n\Delta\tau)$ must be fulfilled. The matching conditions yield a high-dimensional system of $2m(n-1)$ coupled equations, which can be solved by a Newton method. For a typical size of the space-time lattice with $m = 64$ and $n = 151$ used in our calculations the Jacobian matrix in Newton's method has the dimension 19200×19200 , which means about 3.7×10^8 matrix elements. However, the matching

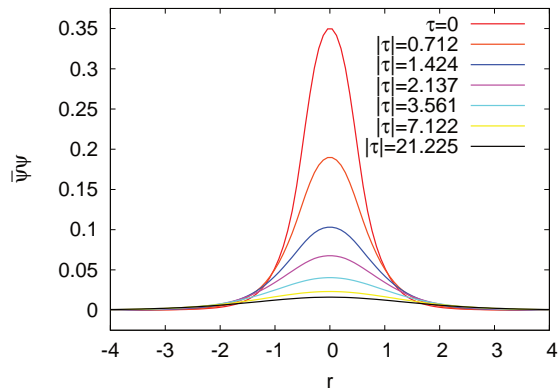


FIG. 3. (Color online) Density $[\bar{\psi}\psi](r)$ of a condensate wave function for a periodic trajectory with period $\beta = 42.45$ computed on the space-time lattice at increasing values $|\tau|$ (from top to bottom line) of the imaginary time. The scaled scattering length is $a = -0.9$.

conditions only depend on the grid points at two adjacent time steps, and thus the Jacobian has a well pronounced band structure which allows for an efficient solution of the linear system of equations [21]. Furthermore, the norm conservation can be used to slightly reduce the number of parameters.

Similar as discussed in Sec. III A for the variational calculations we start searching for periodic trajectories on the space-time lattice with a short period β at mean-field energies slightly below the excited state (see Fig. 1) and then increase β . As an example Fig. 3 shows the density $[\bar{\psi}\psi](r)$ of a condensate wave function for a periodic trajectory with period $\beta = 42.45$ computed on the space-time lattice at various values of the imaginary time τ . The wave function is narrowest at the bounce at $\tau = 0$ and becomes broader with increasing time. Note that the area under each curve in Fig. 3 is not the square norm $2\pi \int_0^\infty r^2 \bar{\psi}(r) \psi(r) dr$ and thus not conserved. As discussed above, the bounce trajectory is obtained in the limit $\beta \rightarrow \infty$.

The Euclidean action of a periodic trajectory on the space-time lattice is computed with Eq. (20). The exact value of the frequency ω_0 is obtained by numerically solving the Bogoliubov-de Gennes equations at the stationary ground state as discussed in Refs. [8, 22]. The parameter v_0 is determined with Eq. (32).

IV. RESULTS AND DISCUSSION

We now present and compare the results obtained with the extended variational approach using coupled Gaussian functions and by the numerically exact simulations on space-time lattices. As outlined above the bounce trajectory is approached via periodic trajectories fulfilling the boundary conditions $\bar{\psi}(0) = \psi(0)$ and $\bar{\psi}(\beta/2) = \psi(\beta/2)$ at the turning points in the limit of

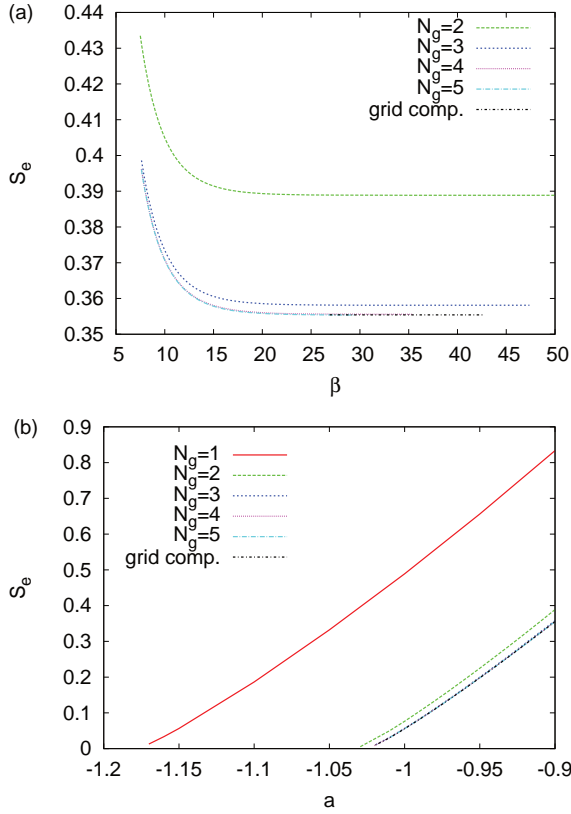


FIG. 4. (Color online) (a) Euclidean action of periodic trajectories at constant scaled scattering length $a = -0.9$. (b) Euclidean action of the bounce trajectory as function of the scaled scattering length a . Shown are the results obtained by the variational approach using up to $N_g = 5$ coupled Gaussians and by numerically exact simulations on grids. The variational results with $N_g > 3$ agree within the line width with the grid computations.

an infinite period $\beta \rightarrow \infty$. The periodic orbit search is started close to the stationary excited state as illustrated in Fig. 1(b) where the period $\beta = 2\pi/\omega_e$ is given by the corresponding stability eigenvalue ω_e of that state. The periodic orbit is then varied towards the bounce trajectory by increasing β in small steps.

The Euclidean action of the periodic orbits at constant scaled scattering length $a = -0.9$ as function of the period β is shown in Fig. 4(a). The results are obtained by the variational approach using up to $N_g = 5$ coupled Gaussians and by numerically exact simulations on space-time lattices. Evidently, the variational calculations converge rapidly to the solution of the numerical grid calculations for an increasing number of Gaussians. For more than three Gaussians the deviations are less than the line widths. However, it is important to note that the converged action deviates significantly from the result obtained with a single Gaussian function [that action is ~ 0.83 for $a = -0.9$ and thus far outside the region presented in Fig. 4(a)]. The action decreases with increasing period, but becomes nearly constant in the re-

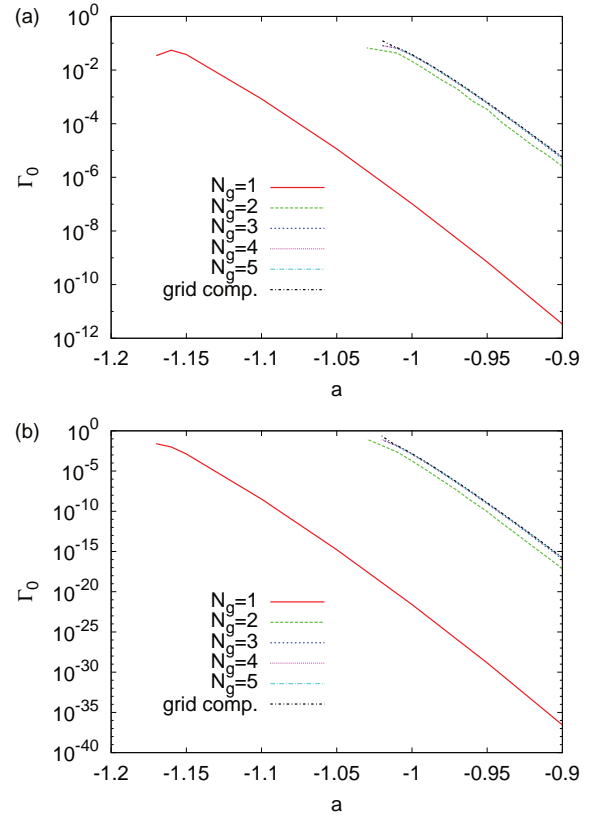


FIG. 5. (Color online) Decay rate by macroscopic quantum tunneling of a BEC with (a) $N = 30$ and (b) $N = 100$ particles obtained by Eq. (8) with the parameters S_b , ω_0 , and v_0 of the bounce trajectory. The variational calculations with $N_g = 1$ to 5 coupled Gaussians converge rapidly to the grid computations, for $N_g \geq 3$ deviations are less than the line width.

gion $\beta \gtrsim 20$, which indicates the rapid convergence to the action of the bounce trajectory.

The limit $\beta \rightarrow \infty$ of the Euclidean action has been estimated for periodic trajectories at various scaled scattering lengths. The resulting action of the bounce trajectory is presented in Fig. 4(b). Again, the variational results converge rapidly to those obtained by simulations on space-time lattices. The action of the bounce trajectory vanishes at the critical scattering length, where the ground and excited state emerge in a tangent bifurcation. The exact critical scattering length is $a_{\text{cr}}^{\text{ex}} = -1.0251$, however, in the variational calculation with a single Gaussian the bifurcation point is significantly shifted to $a_{\text{cr}}^{N_g=1} = -1.1781$. As a consequence in the region $a > a_{\text{cr}}^{\text{ex}} = -1.0251$ the difference between the action obtained with $N_g = 1$ and the exact action is ~ 0.5 , i.e., quite large.

The Euclidean action shown in Fig. 4(b) and the parameters ω_0 and v_0 of the bounce trajectory can now be inserted into Eq. (8) to determine the decay rate Γ_0 of the BEC with attractive $1/r$ interaction. Although particle number scaled units [see Eq. (4)] are used in Eq. (8) the

TABLE I. Decay rates Γ_0 in SI units for self-trapped condensates of $N = 30$ and $N = 100$ ^{87}Rb atoms with the parameters [6, 23] $a_u = \hbar^2/(mu) \sim 2.5 \times 10^{-4}$ m and $t_u = 2ma_u^2/\hbar \sim 27.1$ s.

N_g	$\Gamma_0^{(N=30)}[\text{s}^{-1}]$	$\Gamma_0^{(N=100)}[\text{s}^{-1}]$
1	3.5×10^{-6}	9.65×10^{-20}
2	0.70	0.066
3	1.18	0.45
4	1.21	0.49
5	1.21	0.50
grid	1.21	0.50

decay rate depends, through the replacement $\hbar \rightarrow \hbar/N$ for the macroscopic quantum tunneling of condensates [13], explicitly on the particle number N . As examples, results for a BEC with $N = 30$ and $N = 100$ bosons are presented in Fig. 5(a) and (b), respectively. The decay rate in Eq. (8) is strongly dominated by the exponential term $\exp(-NS_b/\hbar)$. The action of the bounce trajectory tends to zero at the critical value a_{cr} of the tangent bifurcation [see Fig. 4(b)], and therefore macroscopic quantum tunneling can play a non-negligible role at scattering lengths slightly above that value. The variational results in Fig. 5 converge rapidly to those of the grid computations with increasing number of coupled Gaussians. It should be noted that the decay rate obtained with a single Gaussian function deviates in the region $a > a_{\text{cr}}^{\text{ex}} = -1.0251$ from the converged result by about 12 orders of magnitude for $N = 30$ and by about 20 orders of magnitude for $N = 100$ particles.

The decay rates in Fig. 5 are given in particle number scaled dimensionless units. For the experiment proposed by O'Dell et al. [5] experimentally feasible parameters have been found in Ref. [23]. With these values the scattering length and the decay rates can be given in SI units. For ^{87}Rb with $a_u = \hbar^2/(mu) \sim 2.5 \times 10^{-4}$ m and $t_u = 2ma_u^2/\hbar \sim 27.1$ s we present in Table I the decay rates Γ_0 in s^{-1} at scaled scattering length $a = -1$ corresponding to $a^{(\text{SI})} = -a_u/N^2 = -2.78 \times 10^{-7}$ m for $N = 30$ and $a^{(\text{SI})} = -a_u/N^2 = -2.5 \times 10^{-8}$ m for $N = 100$ particles. The values in Table I indicate that the lifetimes of the self-trapped BEC with reasonable experimental parameters can be in the order of seconds at scattering lengths close to the tangent bifurcation. The strong deviations between the decay rates obtained with a single Gaussian function and with improved methods are also evident. Thus, the results presented in Fig. 5 and Table I clearly illustrate that the accurate computation of the bounce trajectory is extremely important for a reasonable quantitative description of macroscopic quantum tunneling.

V. CONCLUSION AND OUTLOOK

We have shown that the exact computation of the bounce trajectory of a BEC using an extended variational approach with coupled Gaussian functions is a full-fledged alternative to numerically expensive simulations on space-time lattices. Very few (about three to five) Gaussians are sufficient to obtain converged results. The method here has been developed for a spherically symmetric self-trapped BEC with an attractive $1/r$ interaction, however, it can straightforwardly also be applied to condensates in an external trap or with a different long-range interaction. The variational approach may be of particular advantage for interactions without spherical symmetry, e.g., in dipolar condensates, which require an increased dimension of the space-time lattice for numerical simulations.

The parameters of the exact bounce trajectory have been used as input in the formula (8) derived by Stoof [13]. This certainly yields improved, however, still not exact values Γ_0 for the decay rate of the BEC by macroscopic quantum tunneling. The reason is that the fluctuations around the stationary ground state and the time-dependent bounce trajectory must be considered, i.e., the decay rates Γ_0 in Eq. (8) must be multiplied with the fluctuation determinant. The computation of the fluctuation determinant and the investigation of macroscopic quantum tunneling in dipolar condensates is work in progress.

The discussions in this paper are based on the mean-field approach for an effective one-particle condensate wave function. For a BEC with attractive interactions and not too many particles effects of depletion can, in principle, be studied beyond the Gross-Pitaevskii theory. In that case the dynamics of the decay should strongly depend on the particle number, in particular for low numbers of particles, and the loss of particles will probably increase the decay. Such computations and comparisons with results obtained within the mean-field approach are an interesting task for future work.

ACKNOWLEDGMENTS

This work was supported by Deutsche Forschungsgemeinschaft.

Appendix A: Gaussian integrals

For the ansatz with real valued coupled Gaussian functions given in Eq. (21) the integrals required in Sec. III A read

$$\langle \bar{g}_l | g_k \rangle = \pi^{3/2} \frac{e^{-\gamma_{kl}}}{A_{kl}^{3/2}}, \quad (\text{A1})$$

$$\langle \bar{g}_l | r^2 | g_k \rangle = \frac{3}{2} \pi^{3/2} \frac{e^{-\gamma_{kl}}}{A_{kl}^{5/2}}, \quad (\text{A2})$$

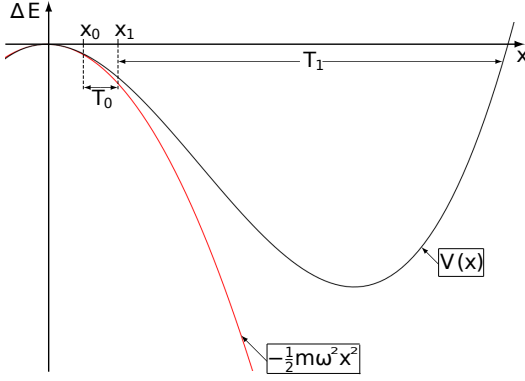


FIG. 6. (Color online) Sketch of a potential with an inverted harmonic saddle at the origin.

$$\langle \bar{g}_l | r^4 | g_k \rangle = \frac{10}{3} \pi^{3/2} \frac{e^{-\gamma_{kl}}}{A_{kl}^{7/2}}, \quad (\text{A3})$$

$$\langle \bar{g}_l | V_c | g_k \rangle = 8\pi^{5/2} a \sum_{i,j=1}^{N_g} \frac{e^{-\gamma_{ijkl}}}{(A_{ijkl})^{3/2}}, \quad (\text{A4})$$

$$\langle \bar{g}_l | r^2 V_c | g_k \rangle = 12\pi^{5/2} a \sum_{i,j=1}^{N_g} \frac{e^{-\gamma_{ijkl}}}{A_{ijkl}^{5/2}}, \quad (\text{A5})$$

$$\langle \bar{g}_l | V_u | g_k \rangle = -4\pi^{5/2} \sum_{i,j=1}^{N_g} \frac{e^{-\gamma_{ijkl}}}{A_{ij} A_{kl} A_{ijkl}^{1/2}}, \quad (\text{A6})$$

$$\langle \bar{g}_l | r^2 V_u | g_k \rangle = -2\pi^{5/2} \sum_{i,j=1}^{N_g} \frac{(2A_{ij} + 3A_{kl}) e^{-\gamma_{ijkl}}}{A_{ij} A_{kl}^2 A_{ijkl}^{3/2}}, \quad (\text{A7})$$

with

$$A_{kl} = A_k + \bar{A}_l, \quad (\text{A8})$$

$$A_{ij} = A_i + \bar{A}_j, \quad (\text{A9})$$

$$A_{ijkl} = A_i + \bar{A}_j + A_k + \bar{A}_l, \quad (\text{A10})$$

$$\gamma_{kl} = \gamma_k + \bar{\gamma}_l, \quad (\text{A11})$$

$$\gamma_{ijkl} = \gamma_i + \bar{\gamma}_j + \gamma_k + \bar{\gamma}_l. \quad (\text{A12})$$

Appendix B: Calculation of v_0

For the calculation of v_0 we assume a potential $V(x)$ with an inverted harmonic saddle at the origin as illustrated in Fig. 6. The period of a trajectory at energy $\Delta E < 0$ is written as $T(\Delta E) = 2(T_0 + T_1)$, with T_0 the time in the region $[x_0, x_1]$ where the harmonic approximation is valid (see Fig. 6). We obtain

$$\begin{aligned} T_0 &= \int_{x_0}^{x_1} \frac{dx}{\dot{x}} = \frac{1}{\omega} \int_{x_0}^{x_1} \frac{dx}{\sqrt{x^2 - x_0^2}} \\ &= \frac{1}{\omega} \cosh^{-1} \frac{x_1}{x_0} \underset{x_0 \ll x_1}{\approx} \frac{1}{\omega} \ln \frac{2x_1}{x_0} \\ \Rightarrow T(\Delta E) &= 2(T_0 + T_1) \approx \frac{2}{\omega} \ln \left(\frac{2x_1}{x_0} e^{\omega T_1} \right). \end{aligned} \quad (\text{B1})$$

When the turning point $x_0 = \sqrt{-2\Delta E/m\omega^2}$ and the point x_1 given by [see Eq. (11)]

$$x_1 = x(T_1) = \frac{v_0}{\omega} e^{-\omega T_1}, \quad (\text{B2})$$

are inserted, Eq. (B1) yields

$$\begin{aligned} T(\Delta E) &\approx \frac{2}{\omega} \ln \left(\frac{2v_0}{\omega x_0} \right) = \frac{1}{\omega} \ln \left(\frac{2mv_0^2}{-\Delta E} \right) \\ \Rightarrow v_0 &= \sqrt{\frac{-\Delta E}{2m}} e^{\omega T/2}. \end{aligned} \quad (\text{B3})$$

With $T = \beta$, $\omega = \omega_0$, $\Delta E = E_{\text{mf}}^g - E_{\text{mf}}(\beta)$, and taking the limit $\beta \rightarrow \infty$ to approach the bounce trajectory we end up with Eq. (32).

-
- [1] M. H. Anderson, J. R. Ensher, M. R. Matthews, C. E. Wieman, and E. A. Cornell, *Science* **269**, 198 (1995)
 - [2] C. C. Bradley, C. A. Sackett, J. J. Tollett, and R. G. Hulet, *Phys. Rev. Lett.* **75**, 1687 (1995)
 - [3] K. B. Davis, M. O. Mewes, M. R. Andrews, N. J. van Druten, D. S. Durfee, D. M. Kurn, and W. Ketterle, *Phys. Rev. Lett.* **75**, 3969 (1995)
 - [4] T. Lahaye, C. Menotti, L. Santos, M. Lewenstein, and T. Pfau, *Rep. Prog. Phys.* **72**, 126401 (2009)
 - [5] D. O'Dell, S. Giovanazzi, G. Kurizki, and V. M. Akulin, *Phys. Rev. Lett.* **84**, 5687 (2000)
 - [6] I. Papadopoulos, P. Wagner, G. Wunner, and J. Main, *Phys. Rev. A* **76**, 053604 (2007)
 - [7] H. Cartarius, J. Main, and G. Wunner, *Phys. Rev. A* **77**, 013618 (2008)
 - [8] H. Cartarius, T. Fabčić, J. Main, and G. Wunner, *Phys. Rev. A* **78**, 013615 (2008)
 - [9] C. Huepe, S. Mérens, G. Dewel, P. Borckmans, and M. E. Brachet, *Phys. Rev. Lett.* **82**, 1616 (1999)
 - [10] C. Huepe, L. S. Tuckerman, S. Mérens, and M. E. Brachet, *Phys. Rev. A* **68**, 023609 (2003)
 - [11] A. Junginger, M. Dorwarth, J. Main, and G. Wunner, *J. Phys. A: Math. Theor.* **45**, 155202 (2012)
 - [12] A. Junginger, J. Main, G. Wunner, and T. Bartsch, *Phys. Rev. A* **86**, 023632 (2012)
 - [13] H. Stoof, *J. Stat. Phys.* **87**, 1353 (1997)
 - [14] J. A. Freire and D. P. Arovas, *Phys. Rev. A* **59**, 1461 (1999)
 - [15] S. Rau, J. Main, and G. Wunner, *Phys. Rev. A* **82**, 023610 (2010)
 - [16] S. Rau, J. Main, H. Cartarius, P. Köberle, and G. Wunner, *Phys. Rev. A* **82**, 023611 (2010)
 - [17] J. A. Freire, D. P. Arovas, and H. Levine, *Phys. Rev. Lett.* **79**, 5054 (1997)

- [18] L. P. Pitaevskii and S. Stringari, *Bose-Einstein Condensation* (Oxford University Press, 2003)
- [19] P. A. M. Dirac, Math. Proc. Cam. Phil. Soc. **26**, 376 (1930)
- [20] A. D. McLachlan, Mol. Phys. **8**, 39 (1964)
- [21] W. H. Press, S. A. Teukolsky, W. T. Vetterling, and B. P. Flannery, *Numerical Recipes in Fortran, Second Edition* (Cambridge University Press, Cambridge, 1992)
- [22] M. Kreibich, J. Main, and G. Wunner, Phys. Rev. A **86**, 013608 (2012)
- [23] S. Giovanazzi, D. O'Dell, and G. Kurizki, Phys. Rev. A **63**, 031603(R) (2001)